Jämsä-Jounela, Sirkka-Liisa

Simulation study of self-tuning adaptive control for rougher flotation

Published in:
Powder Technology

DOI:
10.1016/0032-5910(92)85005-G

Published: 01/01/1992

Document Version
Peer-reviewed accepted author manuscript, also known as Final accepted manuscript or Post-print

Author's accepted manuscript, published in Powder Technology 69 (1992) 33-46

A SIMULATION STUDY OF SELF-TUNING ADAPTIVE CONTROL FOR ROUGHER FLOTATION

SIRKKA-LIISA JÄMSÄ-JOUNELA

Kemira Oy, Porkkalankatu 3, Box 330, 00101 Helsinki, Finland

ABSTRACT

The properties of different self-tuning algorithms are studied and evaluated with help of a phenomenological dynamic simulator of the flotation process. The problem of controlling a system with constant but unknown parameters is considered. In the beginning the analysis is restricted to discrete time single input single output systems. An explicit algorithm obtained by combining a least squares estimator with a minimum variance regulator computed from the estimated model is analyzed. The corresponding implicit generalized minimum variance algorithm is also tested. A multivariable self-tuning regulator based on the minimum variance strategy is represented. The conclusions are drawn upon these simulation results and on practical experience for the use of these algorithms for flotation control.

Keywords
Phosphate flotation control, Flotation modelling, Self-tuning control, Minimum variance control.

INTRODUCTION

The variables of a flotation plant are generally controlled by means of the methods and devices of conventional process control. However, due to the physical characteristics of flotation, their efficiency is relatively limited. Especially the varying composition of the raw ore is a disturbance input to which the plant should adapt. This together with the low cost and increased availability of advanced computer technology, suggest the use of more sophisticated algorithms for plant control.

Optimal control algorithms via applications of the maximum principle have been derived for control of a flotation cell [1, 2]. To the rougher flotation state feedback control and Kalman filter have been applied [3, 4]. A minimum

variance control has been tested for the zinc recleaning, the control variable being the tailing concentration and the frother feedrate being the manipulated variable. A linear difference model also included the cleaner feed pH. The self-tuning regulator was reported to remain stable under all the tested conditions of the short term experiment unliked the conventional PI-controller and to warrant further development for industrial application [5].

The self-tuning regulator was originally developed for the stochastic minimum variance control problem by Åström and Wittenmark [6]. Since the approach is very flexible with respect to the underlying design method many different extensions have been made. Pole placement self-tuners have been investigated by many authors [7, 8, 9, 10]. A generalized minimum variance algorithm using control costing was developed by Clarke and Gawthrop [11, 12]. The LQG design method is the basis for the self-tuners presented in Peterka and Åström [13]. The basic self-tuning controller structure has been extented for the multivariable case by Borisson [14]. Some further improvements have been suggested by Keviczky and Hetthéssy [15]. A related algorithm with weighting on the control is described by Koivo [16]. A straightforward generalization of this idea is described by Goodwin et al where a different delay was associated with each output [17].

This paper describes the simulation results of the two different self-tuning control algorithms tested for a rougher flotation cell. The corresponding multivariable algorithm based on the minimum variance control strategy is also evaluated. The adaptive algorithms and the simulation software presented in this study have been programmed to operate as modules of the CACSD software package which has been designed specially for flotation process control design. The paper describes also the steady state testing phase in the plant to evaluate the initial values for the simulation study and the simulation results of the dynamic behaviour of this rougher flotation cell.

THEORY OF THE SELF-TUNING REGULATORS

The basic idea

Self-tuning controllers can be divided into two categories, explicit and implicit algorithms. When using an explicit algorithm an explicit process model is estimated. This algorithm can be described by two steps. The first step is to estimate the process model parameters on line. Many different estimation schemes can be used, such as stochastic approximation, least squares, extented and generalized least squares, instrumental variable, and maximum likelihood. In the second step a design method is used to determine the polynomials in the regulator using the estimated parameters from the first step. Examples of control design methods which can be used are minimum variance, linear quadratic, pole placement, and model-following. The block diagram of the explicit self-tuning regulator is presented in Fig. 1. In an implicit algorithm the parameters of the regulator are estimated directly. This can be made possible by a reparameterization of the process model. The block diagram of an implicit self-tuning regulator is illustrated in Fig. 2. [18].

SISO system

Process model

Considering q^{-1} to be the backward-shift operator the process model is given by

$$A(q^{-1})y(t) = B(q^{-1})q^{-(d+1)}u(t) + C(q^{-1})\omega(t) \quad (1)$$

where $\{\omega(t)\}$ is a sequence of independent, Gaussian random variables.

$$A(q^{-1}) = 1 - a_1 q^{-1} - \ldots - a_n q^{-n}$$

$$B(q^{-1}) = b_0 + b_1 q^{-1} + \ldots + b_m q^{-m}$$

$$C(q^{-1}) = 1 + c_1 q^{-1} + \ldots + c_1 q^{-1}$$

The model (1) is called the stochastic autoregressive moving-average model or ARMAX model for short.

Minimum variance control

For regulation of systems with one input, one output, the criterion is to minimize the mean-square error between the output and the desired value r(t). This leads to the following cost function

$$J(t+d+1) = E\{[y(t+d+1) - r(t)]^2\} \quad (2)$$

A control law that minimizes the criterion is called minimum variance control.

Optimal prediction

In order to design the controller which minimizes the criterion (2) a minimum variance predictor $\hat{y}(t+d+1|t)$ over (d+1) steps has to be determined.

The model (1) is first written in the form

$$y(t+d+1) = \frac{B(q^{-1})}{A(q^{-1})}u(t) + \frac{C(q^{-1})}{A(q^{-1})}\omega(t+d+1) \quad (3)$$

The second term in the right hand side of the Equation (3) can be expressed using Mac Lauren series as follows

$$\frac{C(q^{-1})}{A(q^{-1})}\omega(t+d+1) = F(q^{-1})\omega(t+d+1) + \frac{G(q^{-1})q^{-(d+1)}}{A(q^{-1})}\omega(t+d+1) \quad (4)$$

Equation (4) gives an identity

$$C(q^{-1}) = F(q^{-1})A(q^{-1}) + q^{-(d+1)}G(q^{-1}) \quad (5)$$

where

$$F(q^{-1}) = 1 + f_1 q^{-1} + \ldots + f_d q^{-d} \tag{6}$$

$$G(q^{-1}) = g_0 + g_1 q^{-1} + \ldots + g_{\bar{s}} q^{-\bar{s}} \tag{7}$$

and in which $\bar{s} = \max(\deg C - d - 1, \deg A - 1, 0)$.

If follows from the Equation (1) that

$$\omega(t) = \frac{A(q^{-1})}{C(q^{-1})} y(t) - \frac{B(q^{-1})}{C(q^{-1})} u(t-d-1) \tag{8}$$

Using the Equation (8) for $\omega(t)$, Equation (3) may be written as

$$y(t+d+1) = \frac{G(q^{-1})}{C(q^{-1})} y(t) + \frac{F(q^{-1})B(q^{-1})}{C(q^{-1})} u(t) + F(q^{-1})\omega(t+d+1) \tag{9}$$

If follows from the Equation (9) that the predictor over (d+1) steps is thus of the form

$$\hat{y}(t+d+1|t) = \frac{G(q^{-1})}{C(q^{-1})} y(t) + \frac{F(q^{-1})B(q^{-1})}{C(q^{-1})} u(t) \tag{10}$$

Minimum variance control law

Having obtained a solution to the prediction problem an admissable control law has to be determined such that the variance of the output is as small as possible. Substituting the predictor (10) to the criterion equation and minimizing the equation respect to u(t), the control law may be written as

$$u(t) = \frac{C(q^{-1})}{B(q^{-1})F(q^{-1})} r(t) - \frac{G(q^{-1})}{B(q^{-1})F(q^{-1})} y(t) \tag{11}$$

The generalized minimum variance algorithm

A slight generalization of the minimum variance control is the algorithm which includes a term in cost function weighting the control effort. The loss function can be thus introduced by

$$J(t+d+1) = E\{[y(t+d+1) - r(t)]^2 + \lambda u^2(t)\} \tag{12}$$

Following the method above the control law may be expressed as

$$u(t) = \frac{C(q^{-1})r(t) - G(q^{-1})y(t)}{B(q^{-1})F(q^{-1}) + (\frac{\lambda}{b_0})C(q^{-1})} \tag{13}$$

If the weighting λ is set to zero, we have an ordinary minimum variance regulator.

Adaptive minimum variance controller

In the explicit approach, a general model is first fitted to the data and then for each set of estimated parameters a d-step-ahead predictor is evaluated. In implicit method the parameters in the optimal predictor are estimated directly [20].

If the parameters are estimated with the resursive extended least squares method (unit delay) the equations are

$$\hat{\theta}(t) = \hat{\theta}(t-1)+aP(t-1)\phi(t-1)e(t) \qquad 0 < a \leq 1 \tag{14}$$

$$e(t) = y(t) - \hat{y}(t) \tag{15}$$

$$P(t-1) = P(t-2) - \frac{P(t-2)\phi(t-1)\phi(t-1)^T P(t-2)}{1+\phi(t-1)^T P(t-2)\phi(t-1)} \tag{16}$$

where

$$\hat{y}(t) = \phi(t-1)^T\hat{\theta}(t-1) \tag{17}$$

$$\phi(t-1) = [y(t-1),\ldots,y(t-n'),u(t-1),\ldots, u(t-m-1),-\hat{y}(t-1),\ldots,-\hat{y}(t-1)] \tag{18}$$

$$\hat{\theta}(t-1) = [\hat{g}_1(t-1),\ldots,\hat{g}_n(t-1),\hat{\beta}_0'(t-1),\ldots,\hat{\beta}_m'(t-1), \hat{c}_1(t-1),\ldots,\hat{c}(t-1)] \tag{19}$$

$n' = \max(n, 1)$.

$\phi(t-1)$ is the datavector for the parameter updating procedure and $\hat{\theta}(t-1)$ is called the parameter matrix at the time t-1.

MIMO system

Process model

The system (1) is described in the multivariable form as follows

$$A(q^{-1})y(t) = B(q^{-1})u(t-k-1)+C(q^{-1})\omega(t) \tag{20}$$

where k is a time delay, y the output vector, u the input vector and $\{\omega(t)\}$ a sequence independent, equally distributed, random vectors with zero mean value and covariance $E[\omega(t)\omega^T(t)]=R$. The vectors y,u and ω are all of dimension p. The polynomial matrices A, B and C are all of dimension p x p, and they are given by

$$A(z) = I+A_1 z+\ldots+A_n z^n \quad (21)$$

$$B(z) = B_0+B_1 z+\ldots+B_{n-1} z^{n-1},\ B_0 \text{ nonsingular} \quad (22)$$

$$C(z) = I+C_1 z+\ldots+C_n z^n \quad (23)$$

where det B(z) and det C(z) have all their zeros strictly outside the unit disc.

Minimum variance strategy

Let Q be a positively semidefinite matrix and consider the criterion

$$\min_{u(t)} E[y^T(t+k+1)Qy(t+k+1)] \quad (24)$$

where k is the time delay in the process model (20). The strategy which minimizes the criterion (24) asymptotically is called the minimum variance strategy or the one step control.

The solution to this optimization problem is fully documented by Borison [14] and the control law required to minimize the Equation (24) is given as follows

$$\tilde{G}(q^{-1})y(s) + \tilde{F}(q^{-1})B(q^{-1})u(s) = 0 \quad (25)$$

The following identify hold

$$C(z) = A(z)F(z) + z^{k+1}G(z) \quad (26)$$

where

$$F(z) = I + F_1 z +\ldots+F_k z^k \quad (27)$$

$$G(z) = G_0 + G_1 z +\ldots+G_{n-1} z^{n-1} \quad (28)$$

Since A(0) is nonsingular, the polynomical matrices F(z) and G(z) are unique.

$\tilde{F}(z)$ and $\tilde{G}(z)$ are introduced by

$$\tilde{F}(z)G(z) = \tilde{G}(z)F(z) \quad (29)$$

where det $\tilde{F}(z)$ = detF(z) and $\tilde{F}(o)$ = I. The polynomical matrices $\tilde{F}(z)$ and $\tilde{G}(z)$ always exist but they are not unique.

Adaptive minimum variance controller

The process to be controlled is given by Equation (20). The self-tuning algorithm performs identification at each sampling interval. The obtained parameters are then used to compute the control signal.

COMPUTER SIMULATION

Hardware configuration and control system software package

The control software package ONSPEC used in this simulation study has been designed to run 286/386 personal computers and is also available for the DEC VMS environment. The configuration for this study has involved

- UNISYS 386 microcomputer
- 1.0 M bytes RAM memory
- 40 M bytes hard disk
- EGA color graphics board
- EGA monitor

A math co-professor chip and 4 M bytes memory board have been added to the system.

The 6.0 version of ONSPEC control software, used in this study, introduces the use of DOS media and a DOS-type operating environment. Concurrent 6.0 is a multi-tasking, multi-user operating system. It features four virtual consoles through user adjustable windows and can also support external user consoles. In this simulation study, for example, the process is displayed in one window, the simulator coded in FORTRAN is running in another one and the trends are displayed in a third window.

The flotation simulator is modular in structure. Software package contains three main modules, which are the steady state and dynamic calculations modules and the control strategies module.

The steady state module contains the following submodules for the mass and water balance calculations of the flotation cell

- data input
- calculations of the mineral distributions
- calculations of the mass and water balances
- calculations of the mineral overall recoveries and recoveris by size interval
- calculations of the cells residence times
- calculations of the cells overall and size interval flotation rate coefficients

The dynamic calculations module contains the flotation process dynamic simulator. This module contains for example a submodule which gives the possibility to simulate random and deterministic disturbances added to the flotation process manipulated variables.

Control strategies module contains the possibility to simulate different single input single output controllers, expert control, adaptive SISO and MIMO control strategies. Expert control is available through the ONSPEC Superintendent which is a real time expert system. Self-tuning control algorithms have been programmed in FORTRAN using the algorithms described in this paper. Control and manipulated variables are user choosable.

All modules described above are menu-driven by ONSPEC control system software package, which gives flexibility and simplicity for the user interface.

Dynamic model of flotation cell

Described flotation simulator is based on a detailed phenomenological flotation model developed and tested by Bascur [19]. This dynamic model has been shown to represent adequately the behaviour of particles of different mineralogical composition and particle sizes under a wide range of steady state and dynamic operating conditions. In the model, the particle/bubble and water transport description together with the hydrodynamic characteristic of a flotation cell have been linked together to provide a general model which includes all controlled and manipulated variables for control system development. The simulation study described here is based on a simplified dynamic model [21].

The set of equations for a mineralogical species j are written as follows:

$$\frac{dC_j^P}{dt} = \frac{Q_{Feed}C_j^{Feed}}{V_{LP}} - \frac{(Q_E+Q_A\alpha_j^P V_{LP}/V_{BP})C_j^P}{(1+\alpha_j^P)V_{LP}} + \frac{Q_R k_j^R C_j^F}{(1+\alpha_j^F)V_{LP}} - \frac{Q_T C_j^P}{(1+\alpha_j^P)V_{LP}} \quad (30)$$

$$\frac{dC_j^F}{dt} = \frac{(Q_E+Q_A\alpha_j^P V_{LP}/V_{BP})C_j^P}{(1+\alpha_j^P)V_{LF}} - \frac{Q_R k_j^R C_j^F}{(1+\alpha_j^F)V_{LF}} - \frac{Q_C C_j^F}{V_{LF}} \quad (31)$$

Equations 30 and 31 represent the mass balance of mineralogical species j in the pulp and froth volumes, V_{LP} and V_{LF}, respectively. C_j represents the concentration of the species j while the superscripts P and F refer to the pulp and froth. Q_{Feed}, Q_E, Q_R, Q_T and Q_C are the volumetric flowrates of liquid in the feed, entrainment, drainage, tailing, and concentrate. Q_A is the volumetric flowrate of air, while α_j^P, α_j^F, and k_j^R are the rate constants of the species in the pulp, froth and drainage.

In order to quantify the transfer of water at the pulp/froth interface, the flowrates of entrained water Q_E, water draining back Q_R, water leaving the cell with concentrate Q_C and tailings Q_T, have to be balanced. The volume balance of the liquid in the flotation cell yields for the pulp

$$\frac{d}{dt}(V_{LP}) = Q_{Feed}-Q_T-Q_E+Q_R \quad (32)$$

and for the froth

$$\frac{d}{dt}(V_{LF}) = Q_E-Q_R-Q_C \quad (33)$$

where V_{LP} is the volume of liquid in pulp; V_{LF} is the volume of liquid in froth and Q_{Feed} is water entering the cell with new feed.

In order to parametrize the simplified model equations, the general steady state system equations corresponding to Eqs (30-33) were used in the present study to obtain the parameters α_j^P and α_j^F. One needed to have a set of data, C_j^{Feed}, C_j^{MP}, C_j^{MF}, the values of Q_R, Q_C, Q_T, Q_E and Q_A obtained for the water model and to solve for α_j^P and α_j^F. The sets of two nonlinear equations were iteratively solved by Newton-Raphson techniques. An initial guess was made for k_j^R and the system was solved for α_j^F and α_j^P. If the system did not converge the initial guess for k_j^R was modified and the procedure repeated.

EXPERIMENTAL

Flotation plant and its regular control

The main minerals of the Siilinjärvi mine and their average contents are apatite 10%, calcite 14% and dolomite 5%, mica 65%, and other silicates 5%. The average phosphate content is only 4%P_2O_5 which makes the Siilinjärvi deposit one of the lowest grade phosphate deposit exploited in the world. The distribution of apatite is relatively constant throughout the deposit, whereas the other minerals, especially carbonates and mica, are more variable. Due to the variation of the latter components, the ore processing is complex and requires a systematic variation of the grinding and flotation conditions according to the ore types.

In the concentrator, there are two parallel, two-stage grinding lines with a capasity of 800 t/h. The total annual capasity is 7.0 million tons. Each circuit comprises a rod mill in open circuit and a ball mill in closed circuit with two-stage hydraulic classification including hydrocylones and cone classifiers.

The mineral pulp is conducted from conditioning to rougher flotation. Rougher concentrates are pumped to a four-stage cleaner flotation circuit. Cleaner circuits are closed, each cleaner tailing reporting to the preceding flotation stage.

The concentrator is extensively automated with the fully distributed microprosessor based system Damatic. All measurements and control actions proceed through the Damatic system. The reporting and process studies are based on a PDP 11/23+ process computer.

Flotation reagents, i.e. the emulsifier, calcite depressant and collector are added to the conditioner and the frother to the rougher flotation feed. There are feedforward control loops which relate the reagent additions to the ore feed with a delay in order to compensate for the variations in throughput.

The slurry levels in the pump sumps are measured by pressure transducers and controlled by the speed of the variable frequency drive pumps. The cell levels are controlled by tail valves and have an additional feedforward compensation from the level of the first cell to the subsequent tail valves.

The flow of the rougher concentrate is controlled by aeration and by frother and emulsifier feeds. If a froth overloading appears, the operator increases depressant feed and may decrease collector feed by changing the setpoint of its controller. The final concentrate flowrate and assay are controlled usually through the air flowrate to the cleaning sections, especially to the fourth cleaner or more seldom through the froth height or reagent feeds. The on-line Courier 40 analyzer has been installed at the plant lately. The rougher flotation process with its instrumentation is shown in Fig. 3.

Steady state model of flotation cell

Since most parameters of the dynamic model are also present in the steady state model, the latter state was first submitted to a study. In addition to collection of the physical and mineralogical data which characterized the ore and the flotation devices, the values of the adjustable quantities like the mass flows, feeds of chemicals, pulp levels and aeration rates were recorded and held constant during a test. Samples were taken from the slurry in the rougher flotation bank (Fig. 3), especially at its second cell which was chosen the particular test object, and analyzed for their particle size distributions and mineral contents.

Although the chemical variations of the natural minerals cause inaccuracies in the different mineral distribution calculations according to their theoretical equations the results of the test No 1 and 2 in Tables I and II, characterize in detail the behaviour of the flotation cell which measured 3.49 m in length, 3.64 m in width and 3.35 m in height. The cell was assumed a perfect mixer and therefore it was modeled in steady state by Eq. (34).

$$Q_T C_j^P = \frac{Q_{Feed} C_j^{Feed}}{1 + k_j \tau} \qquad \tau = \frac{V}{Q_T} \qquad (34)$$

The flotation rate coefficients were calculated from the above equation (Table III). V is the total pulp volume which includes some air and therefore the calculated values of the coefficients are somewhat smaller than their real values.

It is seen from Tables I and II that the apatite and to some degree the calcite and dolomite are concentrated by the cell. Dependence on the particular steady state is shown by the overall rate coefficients of apatite in the two tests which were 0.257 min^{-1} and 0.332 min^{-1} respectively, while the mean residence times were 1.76 min and 1.71 min.

The k's of the different size classes of apatite, calcite and dolomite are shown in Table III. Their dependences on the particle size have a similar form which e.g. indicates losses of the minerals in coarse and to some degree in finest size classes. Substitution of the test data in the model formulae yields then the values of their adjustable factors [22].

A number of other dependences needed by the stated detailed model were determined through separate tests. Several of these were related to the effects of feed and concentration of frother and to the effects of aeration. After the dependence of the surface tension on the frother added had first been determined, it turned out in another test that the power consumption of the impeller was a decreasing function of the aeration. The effects of aeration and frother on the air hold-up were determined indirectly by changing them stepwise and recording the change of pulp level, while the cell level control was disconnected. Bubble sizes and their distributions were determined by means of image recording and analysis techniques.

TABLE I Test run No 1

Stream name	Total flow (t/h)	Dry flow (t/h)	Solids (%)	Assay (P_2O_5)
Cell feed	1885.6	584.0	31.0	2.8
Cell tail.	1811.8	560.0	30.9	2.0
Cell conc.	73.8	24.0	32.6	20.5
	Minerals flows (t/h)			
	Apatite	Calcite	Dolomite	Other
Cell feed	37.99	133.79	89.26	322.99
Cell tail.	26.15	127.06	85.91	320.86
Cell conc.	11.84	6.73	3.35	2.13
	Mineral distribution (%)			
	Apatite	Calcite	Dolomite	Other
Cell feed	6.50	22.91	15.28	55.31
Cell tail.	4.67	22.69	15.34	57.30
Cell conc.	49.23	27.98	13.98	8.86
	Apatite Recovery (%)	Calcite Recovery (%)	Dolomite Recovery (%)	
Cell performance	31.17	5.03	3.75	
Size recovery				
+500 µm	0.33	0.05	0.04	
-500/+210 µm	9.02	1.46	1.09	
-210/+149 µm	20.55	3.32	2.48	
-149/+74 µm	32.40	5.23	3.90	
-74/+37 µm	45.71	7.38	5.51	
-37 µm	53.49	8.63	6.44	

TABLE II Test run No 2

Stream name	Total flow (t/h)	Dry flow (t/h)	Solids (%)	Assay (P_2O_5)
Cell feed	1673.8	545.7	32.6	7.62
Cell tail.	1587.8	500.2	31.5	5.77
Cell conc.	86.0	45.5	52.9	27.70
	Minerals flows (t/h)			
	Apatite	Calcite	Dolomite	Other
Cell feed	99.1	94.7	65.6	286.3
Cell tail.	68.8	86.5	59.4	285.5
Cell conc.	30.3	8.2	6.2	0.8
	Mineral distribution (%)			
	Apatite	Calcite	Dolomite	Other
Cell feed	18.16	17.35	12.03	52.46
Cell tail.	13.70	19.04	12.13	55.13
Cell conc.	66.62	17.99	13.73	1.66
	Apatite Recovery (%)	Calcite Recovery (%)	Dolomite Recovery (%)	
Cell performance	30.60	8.65	9.52	

TABLE III Residence times and flotation rate coefficients for the cell 2220

Residence time 1.76 min and 1.71 min Overall apatite flotation rate coefficient 0.257 and 0.332 min^{-1}			
Size by size flotation rate coefficients in test run 2			
	Apatite (min^{-1})	Calcite (min^{-1})	Dolomite (min^{-1})
+500 µm	0.0000	0.0000	0.0000
-500/+210 µm	0.0124	0.0011	0.0004
-210/+149 µm	0.0298	0.0027	0.0010
-149/+74 µm	0.0657	0.0152	0.0057
-74/+37 µm	0.2393	0.0220	0.0082
-37 µm	0.5847	0.0536	0.0200

Dynamic responses of the cell

In order to study the dynamics of the flotation cell its model was subjected to step tests with aeration rate, collector addition rate, frother addition rate and cell level setpoint. The initial data used for simulations were collected in the beginning of each experiment from the rougher flotation bank and calculations made as described earlier in this text. The dynamic responses were then used to determine the manipulated and controlled variables for the different self-tuning algorithms and to choose the right dynamic model order for the calculations.

Collectors, activators and depressants affect the chemical environment of the flotation pulp and either enhance or reduce the probability of bubble-mineral aggregates being formed. Variables such as froth depth and air addition rate affect the retention time of mineral particles in the froth.

Change in the addition rate of collector may have several effects on the mineral flotation rate depending on the conditions of the pulp and froth before the change is made. An increase in the addition rate of collector may either increase or decrease recovery and concentrate grade depending on the initial collector addition rate. It has been, however, found experimentally that a linear relationship exists between the collector rate and the slow floating fraction of valuable mineral. The physical significance of this relationship relates to the fact that the function of collector in flotation is to render the valuable particles hydrophobic and therefore amenable to flotation, and that it does this by transforming the valuable mineral into fast floating particles. As more collector is added to the process, more valuable minerals are transformed to fast-floating particles until the recovery plateau is received. Change in collector addition rate also causes a change in the behaviour of each size range so slow-floating fraction is also a function of particle size.

Simulated responses in grade and recovery to a change of +5.5 ml/s in the collector flowrate are displayed in Fig. 4. This change is about 25% of the collector addition operating range at the plant. The responses of this rougher flotation cell show that the recovery increases from 31.2 to 33.0% P_2O_5 and the grade increases from 20.1 to 21.9% P_2O_5. The responses show the similarities as reported in [24].

The stability of the froth depends on the amount of frother added. If frother addition rate is increased, the froth becomes more stable and the transfer rate from the froth to the concentrate launder increases. In general the effect of an increase in frother is similar to a decrease in froth height in that it increases the flowrate of water to the concentrate. In Fig. 5 the simulated responses of grade and recovery to a change in frother addition rate are represented. The frother was decreased from 15.3 10^{-6} to 9.6 10^{-6} mol/l, which is about 30% of the frother addition operating range at the plant. The grade difference in steady state is 1.2% P_2O_5 and the recovery difference -2.2% P_2O_5. The pattern of the recovery responses is similar to that represented in [23, 25].

Change in air addition rate at normal levels of aeration has a similar overall effects as a change in froth depth. Decrease in air flowrate increases concentrate grade and decreases recovery of the valuable minerals, because the air affects the flowrate of water to the concentrate and this results in

a proportionally greater reduction of the flowrate of gangue to the concentrate than of that of the valuable mineral. The flotation process responds much faster to changes in aeration rate than to those in froth depth, and aeration rate is often more effective than froth depth in maintaining stable circuit behavior [23].

Simulated responses of grade and recovery to a change of +720 Nm^3/h in total rougher flotation aeration rate are displayed in Fig. 6. In this experiment the grade decreases about -1.2% P_2O_5 and recovery increases about 2.8% P_2O_5.

These three step change tests described above were performed in the operating conditions of Table I.

Froth height affects the residence time in the froth phase and consequently the particle drainage from the froth. The latter feature applies particularly to the gangue particles which generally appear in the froth entrainment. Therefore froth height can be used to control concentrate or tailings grade from a particular bank. Increase of the froth height produces a higher concentrate grade, but at the expense of a loss of recovery. Fig. 7 shows the simulated responses to a froth height change produced by a pulp level setpoint change of -7 cm in the cell. The froth height has thereby been increased by 50% to its operating maximum value. The grade increases producing a steady state difference of about +0.5% P_2O_5 and the recovery increases resulting in a steady state difference of +2.0% P_2O_5. The operating conditions of this step change test are described in Table II.

SIMULATION RESULTS OF THE SELF TUNING REGULATORS

SISO self tuning regulators

Explicit algorithms

In the beginning of the simulation study the SISO self tuning regulators were tested. The first application was the system in which the recovery was chosen to be as output and the air addition rate as input or manipulated variable. The second order model structure with a unit delay was chosen according to the step change tests described earlier in this paper. The recursive least square estimation method was used with the minimum variance control method. The recovery setpoint was in the beginning 30.2% P_2O_5 and the setpoint change was made to a value of 31.2% P_2O_5 at t=480 s. No disturbance was added to the system. The air flowrate was in the beginning 365.5 Nm^3/h, +0.5 Nm^3/h above the steady state value. Testing this basic self-tuning controller the output of the minimum variance controller was not able to follow the reference signal because the bursting problem of parameters. The parameters windup was removed using the constant trace recursive parameter estimation method [26]. The initial covariance matrix P was the I-matrix, the parameters of θ had the values of 0. The variable a(t), which introduces a dead zone in the estimator had a value of 0.5. Because this still resulted in a constant steady state error of -0.5% P_2O_5, the integrator was introduced in the loop. Fig. 8 shows that the new setpoint value was obtained smoothly, no deviation was observed. The response is, however, slow because of the first setpoint change of the experiment. The grade was decreased during the experiment from the value of 27.14% P_2O_5 to a value of 25.62

P_2O_5%. The air flowrate increased from 365.5 to 396.17 Nm^3/h. Minimum limit of the air flowrate was 355.0 and the maximum limit 400 Nm^3/h. In Fig. 9 the results of the simulation in which the reference value is subject to step changes at T = 100 s, 700 s, 1300 s, 1900 s, 2500 s and 3100 s are presented. This simulation gives more information of this adaptive algorithm behavior. Because no special excitation is used in the input variable, the controller convergence to a new setpoint value is slow in the beginning of the simulation. The convergence rate is faster in the last step change of the simulation due to more information of the process dynamics.

The second SISO self-tuning control application was the grade control by the frother addition rate, which is used at the plant when the collector has the optimum value but the grade increase is desired. The same STR-method was used as described above. The initial covariance matrix P was set to αI, where α was 4.0. The initial parameters values of θ were 0. In Fig. 10 the results of the simulation in which the reference value is subject to step changes of +/- 0.5% P_2O_5 at 600s period are presented. The minimum limit of the frother was $3 \cdot 10^{-6}$ mol/l and the maximum limit was $10 \cdot 10^{-6}$ mol/l. The responses of the Fig. 10 show that the increase of $2.2\ 10^{-6}$ mol/l in the frother addition rate produce the increase of +0.5% P_2O_5 in grade but produce the interaction of -0.7% P_2O_5 in recovery. The behaviour of the controller is seen to be satisfactory. However, the limit on control changes may be required if the industrial application is considered.

Implicit algorithms

The generalized minimum variance algorithm was also tested. The first application was the grade control by the collector addition rate and the second application the recovery control by the air flowrate. Recursive parameter estimation was done with the generalized least squares algorithm. Throughout the simulation Gaussian random noise with zero mean value and variance of 0.1 was added to the controlled variables.

In the first test shown in Fig. 11 the grade was chosen as the controlled variable and the collector addition rate as the manipulated variable. The experimental conditions are the same as in the simulations described earlier. The initial collector addition rate was 66.0 ml/s. The initial covariance matrix P was set to αI, where α was 1000. The initial values of θ had the values of 0. The control weighting λ was 0.01. The reference value was subject to step changes of +/- 0.5% P_2O_5 at 600s intervals. Fig. 11 shows that good performance was obtained. No offsets or overshoots was observed.

Fig. 12 repeats the experimental conditions of Fig. 11. The recovery is the output variable and the air flowrate the input variable. The recovery is subject to step changes at the time interval of 600 s. The control weighting can thus be seen to produce better control performance than obtained by the explicit algorithm.

MIMO self-tuning regulator

The simulations were made testing the multivariable minimum variance self tuning controller introduced by Borisson [14]. The controlled variables were the concentrate grade and recovery. The air flowrate and the collector addition rate were chosen as the manipulated variables. The results of the simulations are shown in Fig. 13 and 14.

The reference value of grade is subject to step changes of +/- 0.5% P_2O_5 at T = 100 s, 700 s, 1300 s, 1900 s, 2500 s and 3100 s in the simulation presented in Fig. 13. The maximum limit of the air flowrate was 414 Nm^3/h and the minimum limit 342 Nm^3/h. The limits of the collector addition rate were respectively 60 ml/s and 72 ml/s. The Fig. 13 shows that the setpoint changes of this controlled variable have produced satisfactory responses while the other controlled output, recovery has simultaneously remained close to the desired constant value.

In Fig. 14 the results of the simulation in which the other reference value, recovery was subject to step changes of +/- 0.5% P_2O_5 at the time interval of 600 s are represented. The new setpoint values were reached satisfactorily and only small deviations were observed in the other controlled variable.

CONCLUSIONS

This paper evaluates by simulation the performance of two different self-tuning algorithms based on the minimum variance control strategy. The corresponding multivariable algorithm is also tested.

The simulation results of the SISO self-tuning regulators show that the best control performance has been achieved using the implicit generalized minimum variance algorithm. On advantage with this implicit algorithm over the explicit algorithm can be seen to be also that the design computations are eliminated, since the controller parameters are estimated directly. The implicit algorithm has, however, more parameters to estimate than the explicit algorithms especially if there are long time delays in the process. The implicit algorithms usually have, however, the disadvantage that all process zeros are cancelled. This implies that the implicit methods are intended only for processes with a stable inverse or minimum phase systems. Sampling of a continuous time system often gives a discrete time system with zeros on the negative real axis, inside or outside the unit circle. Cancellation of these zeros will cause more ringing in the control signal. Many implicit algorithms can, however, be used also if the system is nonminimum phase through a proper choise of parameters and by using as much prior information as possible. This has been verified by the in- creasing number of successful application [18].

The simulation results of the MIMO self-tuning regulator show that the tested control method is able to handle the inherent system interactions in a satisfactory manner. The control results could be make even better using a related algorithm with weighting on the control effort [16]. The tuning of multivariable control is, however, an extremely time consuming process and as an industrial applications the self-tuning controllers need as modern control theory applications in general a supervisory/expert system to keep the controllers safety operative. This system should involve in addition to the

normal limit checks of the manipulated variables, algorithms to handle the start-up procedures, algorithms for excitation, different estimation and control algorithms, a logic when a particular algorithms should be used and an information system to help the inexperienced users at the plant.

ACKNOWLEDGEMENTS

This work was done while the author was a visiging scholar at the Department of Metallurgy, at the University of Utah, USA. The author wishs to thank Associate Prof. K. Rajamani for his kind co-operation in the preparation of this paper. This work was supported from the Academy of Finland and Kemira Oy. This support is gratefully acknowledged.

REFERENCES

1 Niemi, A., J. Maijanen and M. Nihtilä (1974). Singular Optimal Feedforward Control of Flotation. IFAC/IFORS Symp. Optimization Methods-Applied Aspects. Varna, Bulgaria, pp. 277-283.

2 Koivo, H. and R. Cojocariu (1977). An Optimal Control for a Flotation Circuit. Automatica, 13, pp. 37-45.

3 Andersen, R., B. Gronli, T. Olsen, I. Kaggerud, K. Ramslo and K.Sandvik (1981). An Optimal Control System of the Rougher Flotation at the Folldal Verk Concentrator, Norway. In J. Laskowski (Ed.). Mineral Processing Proc. 13th Int. Mineral Processing Congress. Vol. II. Elsevier, New York, pp. 1517-1540.

4 Zaragoza, R., and J.A. Herbst (1987). A Model Based Feedforward Control Scheme for Flotation Plants. 116th AIME annual meeting. Denver, Colorado, USA, 23-27 February 1987.

5 Hammoude, A., and H. Smith (1981). Experiments with Self-Tuning Control of Flotation. In O'Shea and Polis (Ed.). Proc. 3rd IFAC Symposium on Automation in Mining, Mineral and Metal Processing. Pergamon Press, Oxford. pp. 213-218.

6 Åström, K.J. and B. Wittenmark (1973). On Self-tuning Regulators. Automatica, 9, pp. 185-199.

7 Edmunds, J.M. (1976). Digital adaptive poleshifting regulators. Thesis, Control systems Centre, UMIS, Manchester, U.K.

8 Wellstead, P.E., J.M. Edmunds, D. Prater and P. Zanker (1979a). Self-tuning pole/zero assignment regulators. Int. J. Control, 30, pp. 1-26.

9 Wellstead, P.E., D. Prager and P. Zanker (1979b). Pole assignment self-tuning regulator. Proc. IEE, 126, pp. 781-787.

10 Åström, K.J. and B. Wittenmark, (1980). Self-tuning controllers based on pole-zero placement. Proc. IEE, 127, 120-130.

11 Clarke, D.W. and P.J. Gawthrop (1975). Self-tuning controller. Proc. IEE, 122, pp. 929-934.

12 Clarke, D.W. and P.J. Gawthrop (1979). Self-tuning control. Proc. IEE. 126, pp. 633-640.

13 Peterka, V. and K.J. Åström (1973). Control of multivariable systems with unknown but constant parameters. Proc. 3rd IFAC Symposium on Identification and System Parameter Estimation, The Hague.

14 Borisson, U. (1979). Self-Tuning Regulators for a Class of Multivariable Systems. Automatica, 15, pp. 209-215.

15 Keviczky, L. and J. Hetthéssy (1977). Self-tuning minimum variance control of mimo discrete time systems. Automatic Control Theory Appl. 5, 11-17.

16 Koivo, H. (1980). A Multivariable self-tuning controller. Automatica, 16, pp. 351-356.

17 Goodwin, G.C., P.J. Ramadge, and P.E. Caines, (1980). Discrete Time Multivariable Adaptive Control; IEEE Transactions on Automatic Control, AC-25, pp. 449-456.

18 Åström K.J. and B. Wittenmark (1989). Adaptive Control, Addison-Wesley, 526 p.

19 Bascur, O.A. (1982). Modelling and Computer Control of a Flotation Cell. Ph.D.Dessertation, University of Utah, Salt Lake City, Utah, USA.

20 Goodwin, G.C. and K.S. Sin (1984). Adaptive Filtering Prediction and Control, Prentice-Hall Information and Systems Science Series. Englewood Cliffs, N.J. 540 p.

21 Bascur, O.A. and J.A. Herbst (1985). On the Development of a Model-Based Control Strategy for Copper Ore Flotation. In E. Forsberg (Ed.). Flotation of Sulphide Minerals. Elsevier, Netherlands. pp. 409-431.

22 Jämsä, S-L. and J.A. Herbst (1988). A Simulation Study of Expert Control System for Flotation. In. J.M. MacLeod and A.D. Heher (Ed.). Software for Computer Control 1988. Pergamon Press, New York, pp. 67-75.

23 Fuerstenau, D.W. (1981). Mineral and Coal Flotation Circuits, Their Simulation and Control. Elsevier Scientific Publishing Company, New York. 291 p.

24 Jämsä-Jounela S-L., Kärki E-K., Expert Control System for Rougher Flotation of Phosphate. IFAC 11th World Congress. August 13-17, 1990, Tallinn, USSR (to appear).

25 Jämsä-Jounela, S-L. and A. Niemi (1989). A Simulation Study of Expert Control System for a Phosphate Flotation Process. 6th IFAC Symposium on Automation in Mining, Mineral and Metal Processing, Buenos Aires, Argentina.

26 Åström, K.J. (1983). Theory and Applications of Adaptive Control - A Survey. Automatica, 19, pp. 421-486.

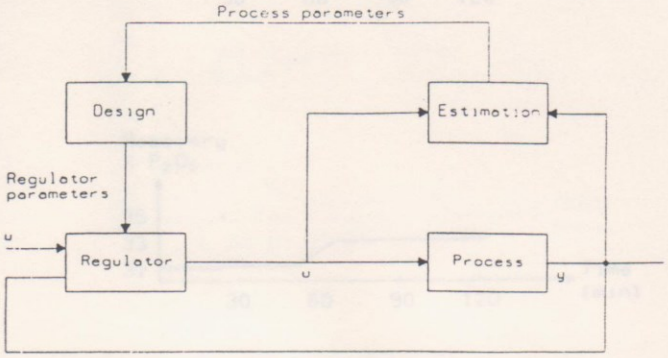

Fig. 1. Block diagram of an indirect self-tuning regulator.

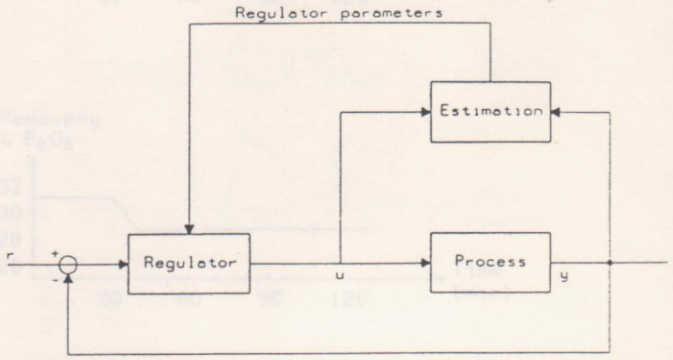

Fig. 2. Block diagram of a direct self-tuning regulator.

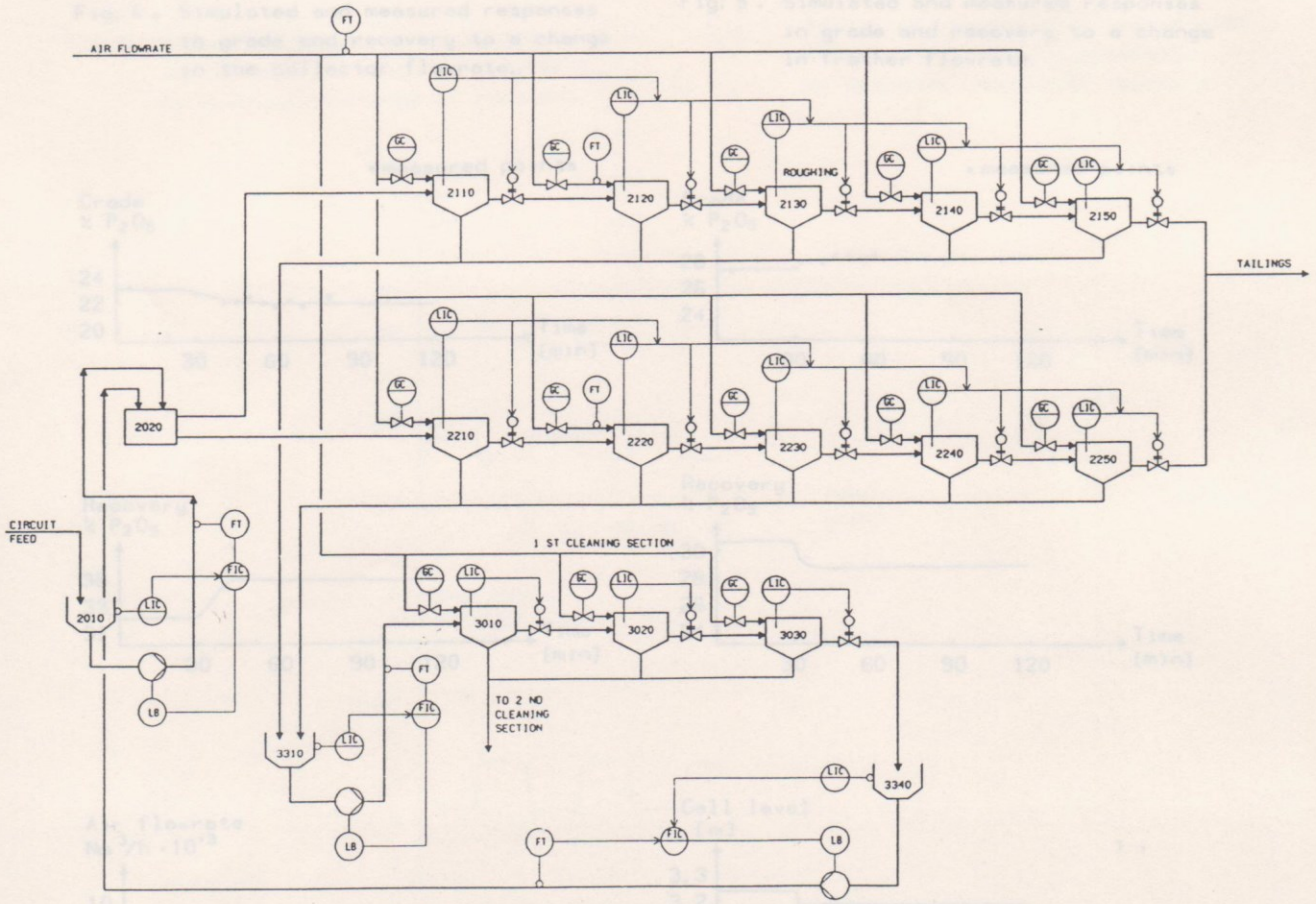

Fig. 3. The rougher flotation circuit at the Siilinjärvi concentrator.

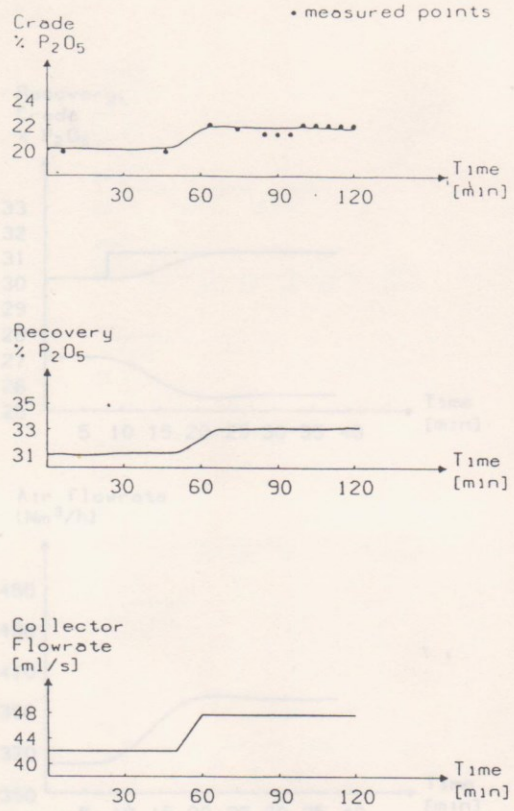

Fig. 4. Simulated and measured responses in grade and recovery to a change in the collector flowrate.

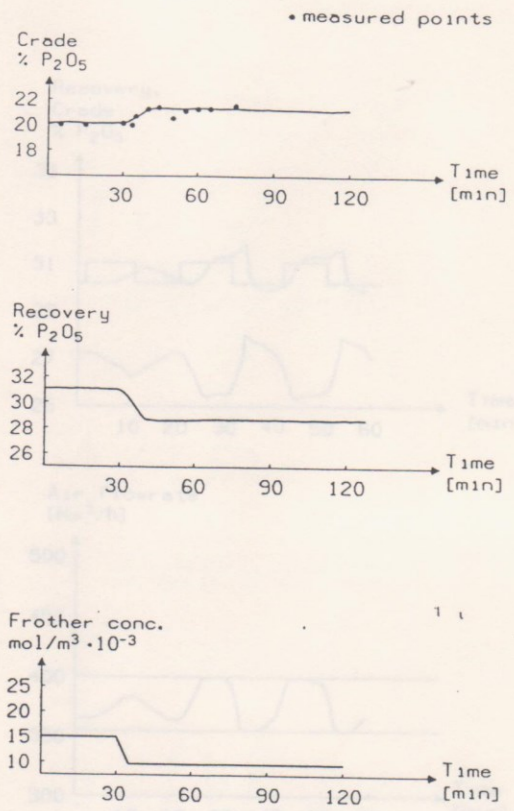

Fig. 5. Simulated and measured responses in grade and recovery to a change in frother flowrate.

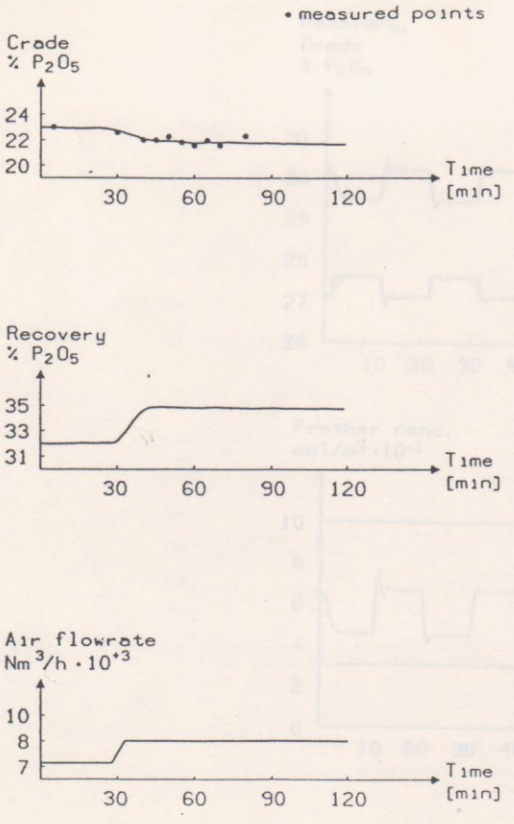

Fig. 6. Simulated and measured responses in grade and recovery to a change in the air flowrate.

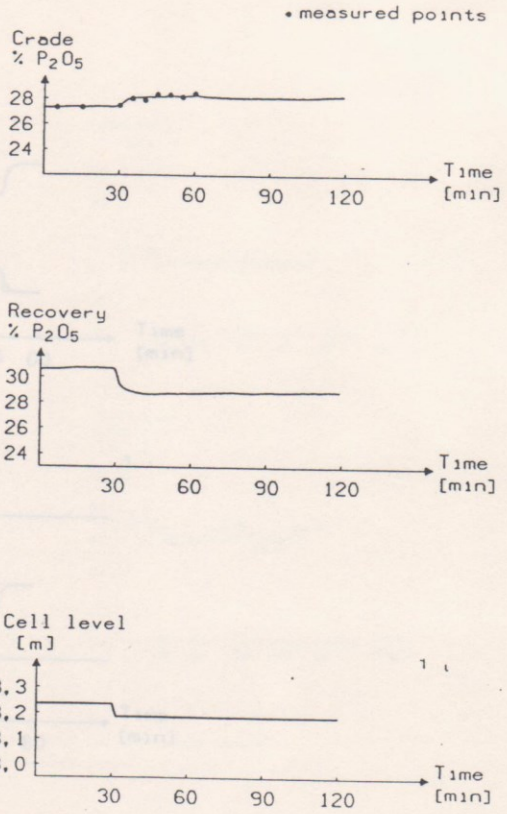

Fig. 7. Simulated and measured responses in grade and recovery to a step change in a cell level setpoint.

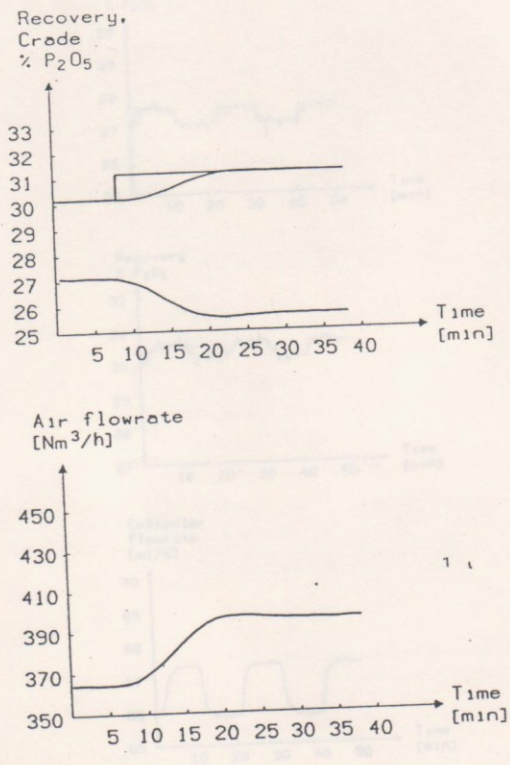

Fig. 8. Simulated responses of system with the minimum variance controller to a setpoint change of recovery.

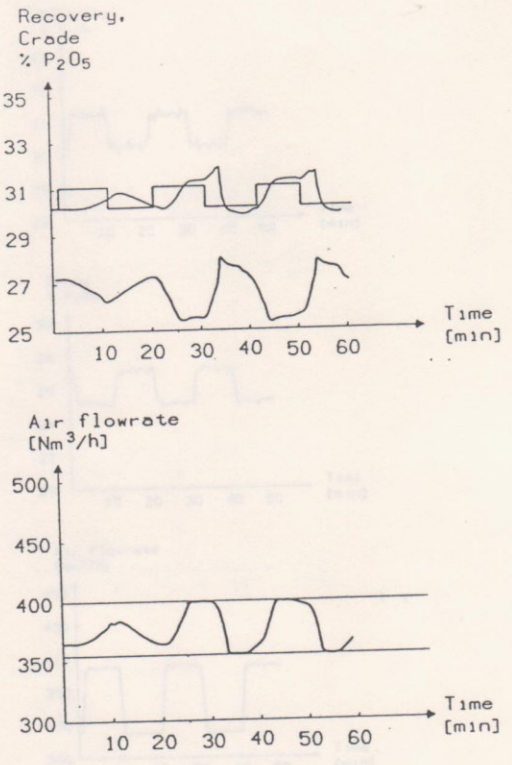

Fig. 9 Simulated responses of system with the minimum variance controller to setpoint changes of recovery.

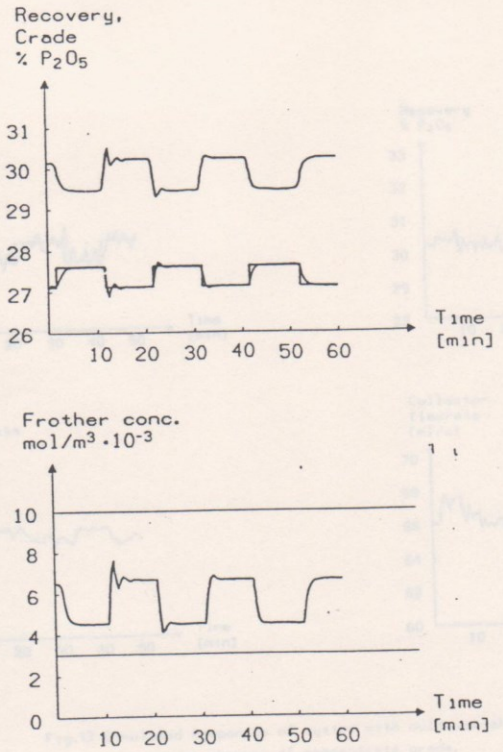

Fig. 10. Simulated responses of system with the minimum variance controller to setpoint changes of concentrate grade.

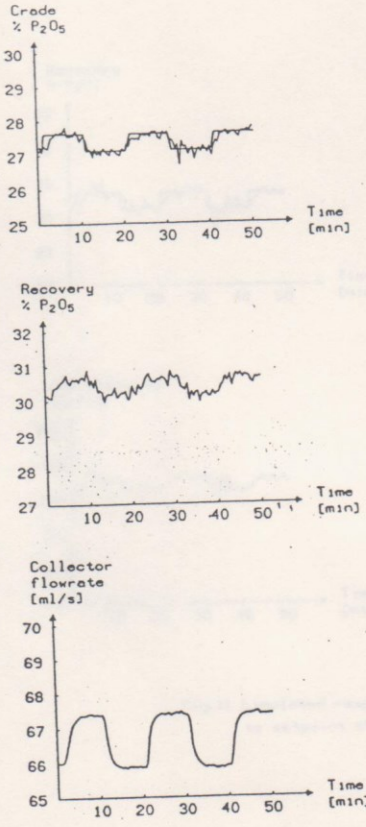

Fig. 11 Simulated responses of system with the generalized minimum variance controller to setpoint changes of concentrate grade.

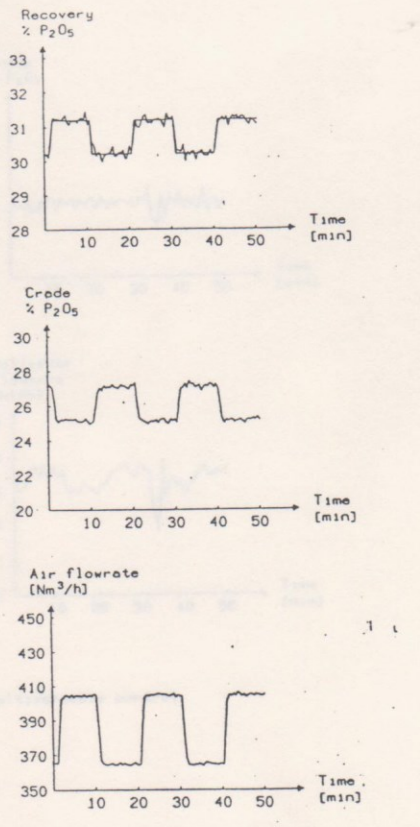

Fig. 12. Simulated responses of system with the generalized minimum variance controller to setpoint changes of recovery.

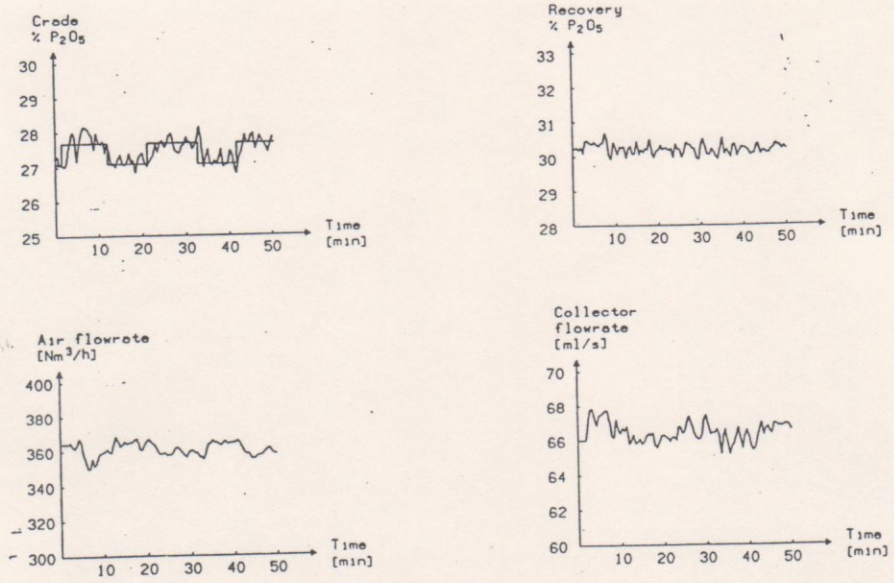

Fig. 13 Simulated responses of system with multivariable control to setpoint changes of concentrate grade.

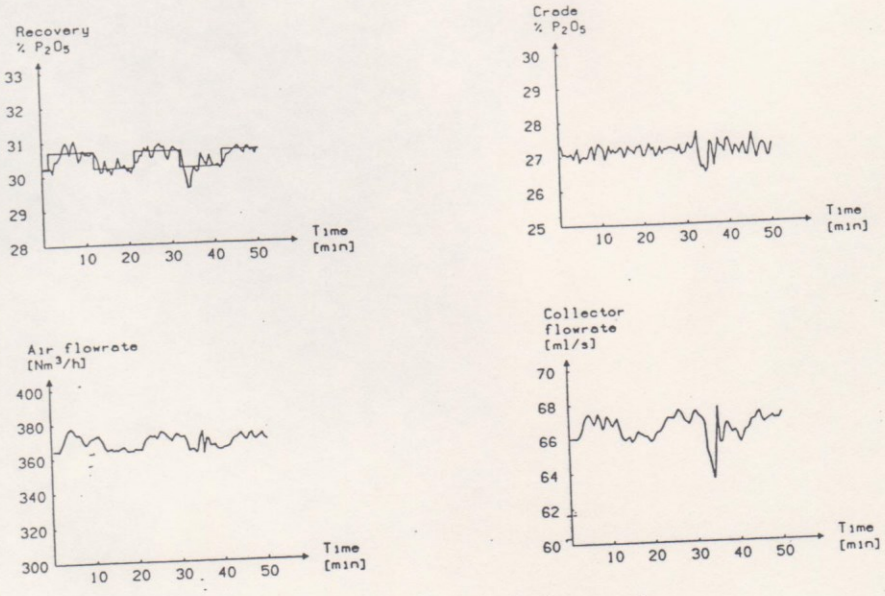

Fig. 14 Simulated responses of system with multivariable control to setpoint changes of recovery.